bioRxiv preprint doi: https://doi.org/10.1101/2022.03.30.486479; this version posted April 1, 2022. The copyright holder for this preprint (which was not certified by peer review) is the author/funder, who has granted bioRxiv a license to display the preprint in perpetuity. It is made available under aCC-BY-NC-ND 4.0 International license.

# The cardiopharyngeal mesoderm contributes to lymphatic vessel development

Kazuaki Maruyama[1, 2, *], Sachiko Miyagawa-Tomita[1, 3, 4], Yuka Haneda[1], Mayuko Kida[1], Fumio Matsuzaki[5], Kyoko Imanaka-Yoshida[2], and Hiroki Kurihara[1, *]

[1]Department of Physiological Chemistry and Metabolism, Graduate School of Medicine, The University of Tokyo, 7-3-1 Hongo, Bunkyo-ku, Tokyo 113-0033, Japan

[2]Department of Pathology and Matrix Biology, Graduate School of Medicine, Mie University, 2-174 Edobashi Tsu, Mie 514-8507, Japan

[3]Heart Center, Department of Pediatric Cardiology, Tokyo Women's Medical University, 8-1 Kawada-cho, Shinjuku-ku, Tokyo 162-8666, Japan

[4]Department of Animal Nursing Science, Yamazaki University of Animal Health Technology, 4-7-2 Minami-osawa, Hachiouji, Tokyo 192-0364, Japan

[5]Laboratory for Cell Asymmetry, RIKEN Center for Developmental Biology, 2-2-3, Minatojiima-Minamimachi, Chuou-ku, Kobe 650-0047, Japan

*Correspondence and requests for materials should be addressed to K.M. (E-mail: k.maruyama0608@gmail.com) and H.K. (E-mail: kuri-tky@umin.net)

## ABSTRACT

Lymphatic vessels are crucial for tissue homeostasis and immune responses in vertebrates. Recent studies have demonstrated that lymphatic endothelial cells (LECs) arise from both venous sprouting (lymphangiogenesis) and de novo production from non-venous origins (lymphvasculogenesis), which is similar to blood vessel formation through angiogenesis and vasculogenesis. However, the contribution of LECs from non-venous origins to lymphatic networks is considered to be relatively small. Here, we identify the *Islet1* (*Isl1*)-expressing cardiopharyngeal mesoderm (CPM) as a non-venous origin of craniofacial and cardiac LECs. Genetic lineage tracing with *Isl1-Cre* and *Isl1-MerCreMer* mice suggested that a subset of CPM cells gives rise to LECs. These CPM-derived LECs are distinct from venous-derived LECs in terms of their developmental processes and anatomical locations. Later, they form the craniofacial and cardiac lymphatic vascular networks in collaboration with venous-derived LECs. Collectively,

bioRxiv preprint doi: https://doi.org/10.1101/2022.03.30.486479; this version posted April 1, 2022. The copyright holder for this preprint (which was not certified by peer review) is the author/funder, who has granted bioRxiv a license to display the preprint in perpetuity. It is made available under aCC-BY-NC-ND 4.0 International license.

our results demonstrate that there are two major sources of LECs, the cardinal vein and the CPM. As the CPM is evolutionarily conserved, these findings may improve our understanding of the evolution of lymphatic vessel development across species. Most importantly, our findings may provide clues to the pathogenesis of lymphatic malformations, which most often develop in the craniofacial and mediastinal regions.

## Introduction

The lymphatic vascular system plays diverse roles in the maintenance of tissue fluid balance, immune surveillance, lipid absorption from the gut, and tumor metastasis[1]. Furthermore, recent progress in molecular and cellular characterization has unveiled the processes involved in the development of the lymphatic vasculature and the roles played by the lymphatic vasculature in various pathophysiological conditions[1–6]. In particular, advances in genetic lineage-tracing and imaging technology have resulted in new findings regarding the embryonic origins and organ-specific roles of the lymphatic vasculature in studies involving mice and zebrafish[7].

The origin of lymphatic endothelial cells (LECs) has been discussed since the 1900s[8,9]. Recent studies using genetic lineage tracing confirmed Sabin's hypothesis that lymphatic vessels originate from the embryonic cardinal vein through lymphangiogenesis[10,11]. In mice, lymphatic vessels arise from the common cardinal vein between embryonic day (E) 9.5 and E10.0 during the partial expression of prospero homeobox transcription protein 1 (Prox1), which is the master regulator of LEC differentiation[10,12]. After that, vascular endothelial growth factor C (VEGF-C) induces the sprouting and expansion of vascular endothelial growth factor receptor 3 $(VEGFR3)^{+}$ LECs from the common cardinal veins to form the first lymphatic plexus[13,14]. This role of venous tissue has also been confirmed in zebrafish[15,16]. In contrast, in tadpoles and avian embryos, mesenchymal cells also contribute to lymphatic vessel development[17–19], supporting Huntington and McClure's suggestion that lymphatic vessels form via the differentiation of mesenchymal cells into LECs, which later develop into a primary lymph sac and connect to the venous system. These findings indicate that there are species-dependent differences in lymphatic vessel developmental processes.

Recent studies involving various mouse genetic lineage-tracing models have revealed that non-venous sources of LECs also contribute to the lymphatic vasculature in the skin,

bioRxiv preprint doi: https://doi.org/10.1101/2022.03.30.486479; this version posted April 1, 2022. The copyright holder for this preprint (which was not certified by peer review) is the author/funder, who has granted bioRxiv a license to display the preprint in perpetuity. It is made available under aCC-BY-NC-ND 4.0 International license.

mesentery, and heart through lymphvasculogenesis[20–25]. Despite the accumulation of studies on non-venous sources of LECs, it remains uncertain how much they contribute to lymphatic vessels throughout the body. Our previous studies showed that LIM-homeodomain protein Islet1 (*Isl1*)-expressing second heart field cells contribute to ventral cardiac lymphatic vessels as a non-venous source of LECs[24]. *Isl1*-expressing second heart field cells have been found to overlap with the progenitor populations that give rise to the pharyngeal muscles in mice and chicks, and they are collectively known as the cardiopharyngeal mesoderm (CPM), which contributes to broad regions of the heart, cranial musculature, and connective tissue[26–29]. Of note, the CPM has been demonstrated to be present in various species, and therefore, it is widely accepted as an evolutionarily conserved mesodermal region[26]. The CPM is composed of the paraxial and splanchnic mesodermal cells surrounding the pharynx. Later, the CPM cells migrate to form the mesodermal cores of the pharyngeal arches. Before their differentiation, CPM cells express both immature skeletal and cardiac muscle markers, including *Isl1*, myocyte-specific enhancer factor 2C (*Mef2c)*, and T-box transcription factor (*Tbx1)*. In mice, these molecules have been shown to be markers of a subset of CPM cells, which play important roles in cardiovascular and skeletal muscle development[26,28–32].

Herein, we identified that the CPM contributes to broader regions of the facial, laryngeal, and cardiac lymphatic vasculature using *Isl1-Cre* and *Isl1-MerCreMer* mice, which can be used to study developmental processes involving the CPM. According to our developmental analysis, CPM-derived progenitor cells have the capacity to differentiate into LECs for a limited embryonic period. CPM-derived LECs are spatiotemporally distinct from venous-derived LECs during the early embryonic period. Later, they coordinate to form capillary lymphatics in and around the cranial and cardiac regions. Conditional knockout (KO) of *Prox1* in *Isl1*-expressing cells resulted in decreased numbers of lymphatic vessels in the tongue and altered the proportions of $Isl1^{+}$ and $Isl1^{-}$ LECs in facial lymphatic vessels. These results suggest that a subpopulation of LECs may share a common mesodermal origin with cardiopharyngeal components. In addition, as the CPM is conserved across vertebrates, they may provide clues regarding the evolution of lymphatic vessel development. In addition, these findings provide a fundamental basis for increasing our understanding of lymphatic vessel development and lymphatic system-related diseases.

bioRxiv preprint doi: https://doi.org/10.1101/2022.03.30.486479; this version posted April 1, 2022. The copyright holder for this preprint (which was not certified by peer review) is the author/funder, who has granted bioRxiv a license to display the preprint in perpetuity. It is made available under aCC-BY-NC-ND 4.0 International license.

## Results

### Isl1$^+$ CPM-derived LECs contribute to cardiac, facial, and laryngeal lymphatic vessel development

To assess the regional contribution of *Isl1*$^+$ CPM cells to lymphatic vessel development, we crossed *Isl1-Cre* mice, which express Cre recombinase under the control of the *Isl1* promoter and in which second heart field-derivatives are effectively labeled, with the transgenic reporter line *R26R-tdTomato* at E16.5. Co-immunostaining of platelet endothelial cell adhesion molecule (PECAM) and vascular endothelial growth factor receptor (VEGFR)3, a lymphatic endothelial cell marker, revealed tdTomato$^+$ LECs in and around the larynx, the skin of the lower jaw, the tongue, and the cardiac outflow tracts at various frequencies, whereas no such cells were found on the dorsal side of the ventricles, which agrees with our previous study [24] (**Figure 1A-H**). We also confirmed that tdTomato$^+$ cells were present in populations of PECAM$^+$ blood and aortic endothelial cells in these regions (**Figure 1A-F**).

To examine whether the *Isl*-marked LECs originated from the neural crest[33], we used *Wnt1-Cre* mice, in which neural crest cells were effectively marked, crossed with the *R26R-eYFP* reporter line. We detected broad eYFP$^+$ cell contributions to the bone, cartilage, and mesenchymal tissues in the head and neck regions as well as the cardiac outflow tract wall, but no eYFP$^+$ LECs were found in these regions (**Figure 1I-O**), excluding the possibility of them originating from the neural crest.

We then investigated the possible contribution of myogenic CPM populations to LECs using *Myf5-CreERT2* mice crossed with the *R26R-tdTomato* line. After tamoxifen was administered at E8.5, tdTomato$^+$ cells were broadly detected in the muscle in the head and neck regions at E16.5, indicating effective Cre-mediated recombination of the target gene. However, no tdTomato$^+$ LECs were detected in the cardiopharyngeal region (**Supplemental Figure 1A-E**). These results indicate that *Isl1*$^+$ CPM cells contribute to broader regions of the LECs in the cardiopharyngeal region.

### Isl1$^+$ CPM cells can differentiate into LECs in a limited developmental period

To determine the timing of the differentiation of CPM into LECs, we employed tamoxifen-inducible *Isl1-MerCreMer* mice crossed with either the *R26R-tdTomato* or *R26R-eYFP* reporter line to conditionally label descendants of *Isl1*-expressing cells. We intraperitoneally injected tamoxifen into pregnant female mice at several timepoints. We

bioRxiv preprint doi: https://doi.org/10.1101/2022.03.30.486479; this version posted April 1, 2022. The copyright holder for this preprint (which was not certified by peer review) is the author/funder, who has granted bioRxiv a license to display the preprint in perpetuity. It is made available under aCC-BY-NC-ND 4.0 International license.

first injected tamoxifen at E6.5 and analyzed the embryos at E16.5 by examining sagittal sections that had been immunostained for PECAM and VEGFR3. We injected tamoxifen into three pregnant female mice; however, due to the toxicity of tamoxifen, we could only obtain two embryos from one mouse. In the embryos, tdTomato$^+$ cells broadly contributed to LECs in and around the larynx, the skin of the lower jaw, the tongue, and the cardiac outflow tracts at various frequencies, but not in the back skin or on the dorsal side of the ventricles (**Supplemental Figure 2A-I**). We then injected tamoxifen at E8.5 and analyzed the embryos at E16.5. Although the contribution of tdTomato$^+$ cells to LECs was smaller, tdTomato$^+$ cells broadly contributed to LECs, as was found for the tamoxifen-treated embryos analyzed at E6.5 (**Figure 2A-H**). In contrast, the number of tdTomato$^+$ LECs seen at E16.5 was markedly decreased when tamoxifen was injected at E11.5 (**Figure 2I-P**). These results indicate that the differentiation of CPM cells into LECs occurs before E11.5.

We then performed whole-mount immunostaining of hearts from E16.5 *Isl1-MerCreMer*;*R26R-eYFP* embryos for PECAM, VEGFR3, and eYFP to show the spatial contribution of *Isl1*$^+$ CPM cells to lymphatic vessels. In the embryos from the mice treated with tamoxifen at E8.5, eYFP$^+$ cells were detected in VEGFR3$^+$ lymphatic vessels around the cardiac outflow tracts. In contrast, we could not detect eYFP$^+$ cells in the VEGFR3$^+$ lymphatic vessels around the cardiac outflow tracts when tamoxifen was administered at E11.5, or on the dorsal side of the ventricles when tamoxifen was administered at E8.5 or E11.5 (**Figure 3A-H**). These results indicate that *Isl1*$^+$ CPM cells gradually lose their capacity to differentiate into LECs as development progresses.

**Isl1$^+$ CPM-derived LECs are spatiotemporally distinct from vein-derived LECs**

We next analyzed the early stages of the spatiotemporal development of *Isl1*$^+$ CPM-derived lymphatic vessels using *Isl1-Cre;R26R-eYFP* mice by performing immunostaining for PECAM, Prox1, and eYFP. At E11.5, eYFP$^+$/Prox1$^+$ cells were detected around the eYFP$^+$ mesodermal core region of the first and second pharyngeal arches in *Isl1-Cre;R26R-eYFP* mice (**Figure 4A and B**). At E12.0, eYFP$^+$/Prox1$^+$ cells were distributed in the pharyngeal arch region and extended toward the lymph sac-forming domain composed of eYFP$^-$/Prox1$^+$ cells, which were considered to emerge from the cardinal vein and intersomitic vessels, as reported previously[11] (**Figure 4C and D**).

bioRxiv preprint doi: https://doi.org/10.1101/2022.03.30.486479; this version posted April 1, 2022. The copyright holder for this preprint (which was not certified by peer review) is the author/funder, who has granted bioRxiv a license to display the preprint in perpetuity. It is made available under aCC-BY-NC-ND 4.0 International license.

At E14.5, eYFP$^+$/Prox1$^+$/PECAM$^+$ LECs formed lymphatic capillaries in the lower jaw and the tongue, which are derived from the first pharyngeal arch (**Figure 4E-G**).

We then analyzed *Isl1-MerCreMer;R26ReYFP* embryos at E12.0. After tamoxifen was administered at E8.5, eYFP$^+$/Prox1$^+$ cells were found in and around the pharyngeal mesodermal condensation, close to the lymph sac-forming region, as was seen in the *Isl1-Cre;R26ReYFP* embryos (**Figure 4H and I**). No eYFP$^+$/Prox1$^+$ cells were observed in or around the cardinal veins (**Figure 4J**). Some of the eYFP$^+$/Prox1$^+$ cells in the pharyngeal arch region expressed PECAM at E12.0, indicating that they had endothelial characteristics (**Figure 4K and L**). After tamoxifen was administered at E9.5, the number of eYFP$^+$/Prox1$^+$ LECs was significantly decreased compared with that seen in the embryos treated with tamoxifen at E8.5 (**Figure 4M-O).** These results indicate that the commitment of *Isl1*$^+$ CPM cells to LEC differentiation occurs before E9.5 in the pharyngeal arch region.

**Loss of Prox1 in Isl1$^+$ lineages reveals the importance of Isl1$^+$ CPM-derived LECs for cranial lymphatic vessel development**

To investigate the functional importance of *Isl1*$^+$ CPM-derived LECs for the development of cranial lymphatic vessels (the lymphatics of the lower jaw skin, cheeks, and tongue), we conditionally knocked out *Prox1* in CPM populations by crossing *Prox1*-flox (*fl*) mice, which expressed eGFP under the control of the *Prox1* promoter upon Cre-mediated exon 2 deletion[34], with *Isl1-Cre* mice. When lymphatic vessel formation in these regions was analyzed in mice that were heterozygous or homozygous for the *Prox1*$^{fl}$ allele, the number and area of VEGFR3$^+$/PECAM$^+$ lymphatic vessels were significantly lower in the tongues of the *Isl1-Cre;Prox1*$^{fl/fl}$ homozygous mice than in those of the *Isl1-Cre;Prox1*$^{fl/+}$ heterozygous mice (**Figure 5A-C, F-H, K, and L**). In contrast, the formation of facial lymphatic vessels in the lower jaw and cheeks was not significantly affected by the deletion of *Prox1* in the *Isl1*$^+$ lineage (**Figure 5D-E’’’, I-J’’’, O, and P**). There were no differences in the mean diameter of the tongue or facial lymphatic vessels between the *Isl1-Cre;Prox1*$^{fl/fl}$ homozygous mice and *Isl1-Cre;Prox1*$^{fl/+}$ heterozygous mice (**Figure 5A-J, M, and Q**). Next, we examined the contribution of the *Isl1*$^+$ lineage to regional lymphatic vessel formation by assessing the relative area of eGFP$^+$ cells among VEGFR3$^+$ LECs to determine whether the regional differences in the effects of *Isl1*$^+$-lineage-specific *Prox1* deletion on lymphatic vessel formation were due to differences in

bioRxiv preprint doi: https://doi.org/10.1101/2022.03.30.486479; this version posted April 1, 2022. The copyright holder for this preprint (which was not certified by peer review) is the author/funder, who has granted bioRxiv a license to display the preprint in perpetuity. It is made available under aCC-BY-NC-ND 4.0 International license.

compensation by other cell sources. *Isl1-Cre;Prox1*$^{fl/+}$ heterozygous mice showed that the *Isl1*$^{+}$ lineage was almost totally responsible for the development of the tongue and facial skin lymphatic vessels (**Figure 5A-E'''', N, and R**). On the other hand, *Isl1-Cre;Prox1*$^{fl/fl}$ homozygous mice showed a lower contribution of the *Isl1*$^{+}$ lineage to the facial skin lymphatics (**Figure 5F, I-J'''', and R**), whereas its contribution to the lymphatic vessels in the tongue was not decreased (**Figure 5F-H and N**). These results suggested that defects in LEC differentiation and/or maintenance due to *Prox1* deletion in the *Isl1*$^{+}$ lineage were compensated for by other cell sources, probably of venous origin, in facial skin, but not in the tongue, resulting in impaired lymphatic vessel formation in the tongue.

**Loss of Prox1 in Tie2$^{+}$ lineages confirms the heterogeneous origins of LECs**

To further investigate the regional differences in the contributions of venous and non-venous cell sources to LECs, we crossed *Prox1*$^{fl}$ mice with endothelial/hematopoietic cell-specific *Tie2-Cre* mice. We immunostained sagittal sections of the resultant embryos for PECAM, green fluorescent protein (GFP), and the LEC marker lymphatic vessel endothelial hyaluronan receptor (LYVE)1 at E16.5, when lymphatic networks are distributed throughout the whole body[10]. We identified LECs by their luminal structure and the colocalization of PECAM and LYVE1, the latter of which is also known to be expressed in a subset of macrophages.

We compared lymphatic vessel development in the tongue, the skin of the lower jaw, and back skin between mice that were heterozygous and homozygous for the *Prox1*$^{fl}$ allele to assess the morphological changes in LYVE1$^{+}$/PECAM$^{+}$ lymphatic vessels seen in each tissue. In the tongue, the number of LYVE1$^{+}$/PECAM$^{+}$ lymphatic vessels was significantly lower and the mean lymphatic vessel diameter was significantly higher in the *Tie2-Cre;Prox1*$^{fl/fl}$ homozygous mice than in the *Tie2-Cre;Prox1*$^{fl/+}$ heterozygous mice (**Figure 6A and B and Supplemental Figure 3A-C**). Almost all of the LYVE1$^{+}$/PECAM$^{+}$ lymphatic vessels in the tongue were positive for eGFP in the *Tie2-Cre;Prox1*$^{fl/+}$ heterozygous mice (**Figure 6A and Supplemental Figure 3D**), indicating that the majority of LECs derived from *Isl1*$^{+}$ CPM cells developed through *Tie2* expression in the tongue. Remarkably, in the tongues of the *Tie2-Cre;Prox1*$^{fl/fl}$ homozygous mice many of the eGFP$^{+}$ cells were not incorporated into the LYVE1$^{+}$/PECAM$^{+}$ lymphatics, resulting in an increased eGFP$^{+}$ area to lymphatics area

bioRxiv preprint doi: https://doi.org/10.1101/2022.03.30.486479; this version posted April 1, 2022. The copyright holder for this preprint (which was not certified by peer review) is the author/funder, who has granted bioRxiv a license to display the preprint in perpetuity. It is made available under aCC-BY-NC-ND 4.0 International license.

ratio (**Figure 6A and B and Supplemental Figure 3D**), which was indicative of impaired differentiation of venous cells into LECs or impaired maintenance of LEC identities due to a lack of Prox1 expression in the *Tie2*$^{+}$ endothelial cells.

On the contrary, compared with that seen in the *Tie2-Cre;Prox1*$^{fl/+}$ heterozygotes lymphatic vessel formation in the lower jaw and back skin was not significantly affected in the *Tie2-Cre;Prox1*$^{fl/fl}$ homozygotes, although the mean vessel diameter in the back skin of the homozygotes was increased (**Figure 6C-F and Supplemental Figure 3E-G and I-K**). In contrast to the tongue, the eGFP$^{+}$ area to LYVE1$^{+}$/PECAM$^{+}$ lymphatics area ratios in the lower jaw and back skin were relatively low in both the *Tie2-Cre;Prox1*$^{fl/+}$ heterozygotes and *Tie2-Cre;Prox1*$^{fl/fl}$ homozygotes (**Figure 6C-F and Supplemental Figure 3H and L**). These results demonstrate that the lymphatic vessels in these regions are composed of *Tie2*$^{+}$ and *Tie2*$^{-}$ LECs, supporting the idea that LECs have heterogeneous origins.

Taken together with the data from the experiments involving *Isl1-Cre* mice, these results suggest that the LECs in the craniofacial region have heterogeneous origins and developmental processes. Specifically, the LECs in the tongue are derived from the *Isl1*$^{+}$/*Tie2*$^{+}$ lineage, whereas the LECs in facial skin, including the skin on the lower jaw, are derived from the *Isl1*$^{+}$/*Tie2*$^{+}$ and *Isl1*$^{+}$/*Tie2*$^{-}$ lineages, which may compensate for each other when LECs from one lineage are impaired. Similarly, the LECs in back skin are derived from the *Tie2*$^{+}$ and *Tie2*$^{-}$ lineages, which may compensate for each other, whereas the *Isl1*$^{+}$ lineage is not involved in the development of these cells.

## Discussion

In this study, we demonstrated that *Isl1*$^{+}$ CPM cells, which are known to be progenitors of the cranial and cardiac musculature and connective tissue, contribute to the formation of lymphatic vessels in the cardiopharyngeal region, including the tongue, facial skin, larynx, and cardiac outflow tracts. We also showed that *Myf5*$^{+}$ myogenic lineages, which were previously suggested to be possible sources of LECs[35], did not contribute to lymphatic vasculature formation in *Myf5-CreERT2* mice subjected to tamoxifen treatment at E8.5. Tamoxifen-inducible genetic lineage tracing further indicated that *Isl1*$^{+}$ CPM-derived progenitors only have the potential to differentiate into LECs before E9.5. In accordance with these findings, *Isl1*$^{+}$ CPM-derived LECs showed distinct spatiotemporal developmental processes and subsequently coordinated with *Isl1*$^{-}$ venous-

bioRxiv preprint doi: https://doi.org/10.1101/2022.03.30.486479; this version posted April 1, 2022. The copyright holder for this preprint (which was not certified by peer review) is the author/funder, who has granted bioRxiv a license to display the preprint in perpetuity. It is made available under aCC-BY-NC-ND 4.0 International license.

derived LECs arising from the lymph sac-forming domain to form the systemic lymphatic vasculature. In addition, conditional KO of *Prox1* in the *Isl1*$^{+}$ lineage resulted in lymphatic vessel deficiencies in the tongue. In contrast, in the facial skin, the loss of *Isl1*$^{+}$ LECs was compensated for by increased numbers of *Isl1*$^{-}$ LECs. Accordingly, conditional KO of *Prox1* in *Tie2*$^{+}$ cells produced regional lymphatic phenotypic differences in the tongue, the skin of the lower jaw, and back skin. These results indicate that the LECs in the cardiopharyngeal region are mainly derived from *Isl1*$^{+}$ CPM progenitors.

The present study further indicates that the LECs in the tongue are derived from *Tie2*-expressing cells among the *Isl1*$^{+}$ lineage. Although it is unclear whether *Isl1*$^{+}$-derived cells at the *Tie2*-expressing stage represent a venous endothelial identity, this result means that *Tie2*$^{+}$ LECs are not equivalent to cardinal vein-derived LECs. Furthermore, *Tie2-Cre;Prox1*$^{fl/fl}$ homozygotes exhibited greater numbers of eGFP$^{+}$/LYVE1$^{-}$/PECAM$^{+}$ cells than *Tie2-Cre;Prox1*$^{fl/+}$ heterozygotes (**Figure 5A-C, 5F-H, and 6A and B**). As a previous study found that conditional KO of *Prox1* could reprogram LECs to become blood endothelial cells (BECs)[36], the number of BECs (eGFP$^{+}$/LYVE1$^{-}$/PECAM$^{+}$ cells) may be increased in the tongues of *Tie2-Cre;Prox1*$^{fl/fl}$ homozygous mice due to impaired maintenance of the LEC identity of *Isl1*$^{+}$ CPM-derived cells that would have normally expressed Prox1. In contrast, the *Isl1*$^{+}$ CPM-derived LECs in facial skin were not labeled by *Tie2-Cre*, indicating that there is heterogeneity within *Isl1*$^{+}$ CPM-derived LECs. Although further studies are needed to examine the phenotypic differences between the LECs in the tongue and facial skin, it is possible that differentiation processes may be affected by the extracellular environment, e.g., through interactions with the surrounding cells and extracellular matrix.

A recent study has suggested that *Pax3*$^{+}$ paraxial mesoderm-derived cells contribute to the cardinal veins, and therefore, venous-derived LECs are *Pax3*$^{+}$. In experiments involving *Myf5-Cre* mice, it was also suggested that the *Myf5*$^{+}$ lineage contributes to LECs in embryonic lymph sacs [35]; however, we could not identify *Myf5*$^{+}$ LECs in *Myf5-CreERT2* mice after tamoxifen treatment was administered at E8.5 (**Supplemental Figure 1**). This discrepancy may have been caused by differences in the mouse lines, the timing of Cre-recombination, the genetic background, or the breeding environment.

Several studies have confirmed that *Isl1*$^{+}$ LECs contribute to the ventral side of the heart[24,25]. In a retrospective clonal analysis of mouse embryos, Lescroart et al. showed

bioRxiv preprint doi: https://doi.org/10.1101/2022.03.30.486479; this version posted April 1, 2022. The copyright holder for this preprint (which was not certified by peer review) is the author/funder, who has granted bioRxiv a license to display the preprint in perpetuity. It is made available under aCC-BY-NC-ND 4.0 International license.

297 that there were distinct sublineages within the myogenic progenitors in the CPM [32]. The
298 first pharyngeal CPM contributes to the temporalis and masseter muscles and the right
299 ventricle, whereas the second pharyngeal CPM contributes to broad regions of the facial
300 muscles and the bases of the cardiac outflow tracts[32]. Milgrom-Hoffman et al. identified
301 $Flk1^{+}/Isl1^{+}$ endothelial populations in the second pharyngeal arch in mouse embryos from
302 E7.5 to E9.5[37]. These cell populations may serve as progenitors for LECs and BECs in
303 the cardiopharyngeal region through the sequential expression of *Flk1*, *Tie2*, and/or *Prox1*
304 in response to different cues, leading to diverse fate determination, as revealed by recent
305 single cell RNA-sequence analyses[38,39].
306 Heart development and pharyngeal muscle development are known to be tightly
307 linked, suggesting that these tissues share common evolutionary origins[26,29]. As the CPM
308 is conserved in various species, CPM-derived LECs may also be evolutionarily conserved.
309 In agreement with this, several studies involving zebrafish have indicated that facial and
310 cardiac LECs originate from distinct cell sources from venous-derived LECs[40,41].
311 Lymphatic malformations (LMs) are congenital lesions, in which enlarged and/or
312 irregular lymphatic connections do not function properly. The causes of LMs are
313 unknown, but LMs commonly occur in the head and neck regions[42]. Accumulating
314 evidence has shown that mutations in the *phosphatidylinositol-4,5-bisphosphate 3-kinase*
315 *catalytic subunit alpha* (*PIK3CA*) gene are found more frequently in LECs than in
316 fibroblasts in LM patients[43]. Given the fact that CPM-derived LECs were distributed
317 around the head and neck and were found in the lymph-sac forming domain in the cervical
318 region in the present study (**Figures 1-4**), LMs may be caused by *PI3KCA* mutations in
319 CPM-derived LECs. In addition to LMs, several blood vessel malformations frequently
320 occur in the neck and facial regions. Thus, some types of blood vessel malformations may
321 also be caused by mutations in CPM progenitors.
322 In summary, the present study supports the idea that $Isl1^{+}$ CPM cells are progenitors
323 of LECs, which broadly contribute to cranial, neck, and cardiac lymphatic vessels in
324 concert with venous-derived LECs. These findings are expected to shed new light on the
325 cellular origins of lymphatic vessels and the molecular mechanisms of lymphatic vessel
326 development, which may increase our understanding of the evolution of lymphatic
327 vessels and the pathogenesis of lymphatic system-related diseases.
328
329

bioRxiv preprint doi: https://doi.org/10.1101/2022.03.30.486479; this version posted April 1, 2022. The copyright holder for this preprint (which was not certified by peer review) is the author/funder, who has granted bioRxiv a license to display the preprint in perpetuity. It is made available under aCC-BY-NC-ND 4.0 International license.

## Materials and methods

### Mouse strains

The following mouse strains were used: *Isl1-Cre*[44], *Isl1-MerCreMer*[45], *Wnt1-Cre*[46], *Myf5-CreERT2*[47], *R26R-eYFP*[48], *Rosa26-tdTomato*[49], *Tie2-Cre*[50], and *Prox1*$^{fl/+}$[34]. All mice were maintained on a mixed genetic background (C57BL/6J x Crl:CD1(ICR)), and both sexes were used (the mice were randomly selected). The genotypes of the mice were determined via the polymerase chain reaction using tail-tip or amnion DNA and the primers listed in Table 1. The mice were housed in an environmentally controlled room at 23±2 ˚C, with a relative humidity level of 50–60%, under a 12-h light:12-h dark cycle. Embryonic stages were determined by timed mating, with the day of the appearance of a vaginal plug being designated embryonic day (E) 0.5. All animal experiments were approved by the University of Tokyo and Mie University animal care and use committee, and were performed in accordance with institutional guidelines.

### Immunohistochemistry, histology, confocal imaging, and quantification

For the histological analyses, hearts and embryos were collected, fixed in 4% paraformaldehyde for 1 hour at 4 ℃, and stored in phosphate-buffered saline or embedded in optimal cutting temperature compound (Sakura Finetek, Tokyo, Japan). Immunostaining of 16-μm-thick frozen sections was performed using primary antibodies against CD31 (553370, BD Pharmingen, 1:100), Prox1 (11-002, AngioBio, 1:200; AF2727, R&D Systems, 1:200), LYVE1 (AF2125, R&D Systems, 1:150), VEGFR3 (AF743, R&D Systems, 1:150), and GFP (GFP-RB-AF2020, FRL, 1:500). Alexa Fluor-conjugated secondary antibodies (Abcam, 1:400) were subsequently applied. The same protocol was followed for whole-mounted hearts and embryos, with the primary and secondary antibody incubation periods extended to two nights. Immunofluorescence imaging was conducted using a Nikon C2 confocal microscope or Keyence BZ-700. All images were processed using the ImageJ and Nikon NIS Elements software.

### Tamoxifen injection

For the lineage tracing using the *Isl1-MerCreMer* or *Myf5-CreERT2* lines, tamoxifen (20 mg/mL; Sigma) was dissolved in corn oil. Pregnant mice were injected intraperitoneally with 125 mg/kg body weight of tamoxifen at the indicated timepoints.

bioRxiv preprint doi: https://doi.org/10.1101/2022.03.30.486479; this version posted April 1, 2022. The copyright holder for this preprint (which was not certified by peer review) is the author/funder, who has granted bioRxiv a license to display the preprint in perpetuity. It is made available under aCC-BY-NC-ND 4.0 International license.

363

364 **Statistical analysis**

365 Data are presented as the mean ± standard error of the mean (SEM). Mann-Whitney's *u*-
366 tests was used for comparisons between two groups. *P*-values of <0.05 were considered
367 statistically significant.

368

369 **AUTHORS' CONTRIBUTIONS**

370 K.M., S.M.-T., and H.K. conceived the study and designed the experiments. K.M., Y.H.,
371 and M.K. performed the experiments. F.M. provided the *Prox1*$^{fl/+}$ mice. K.M., S.M.-T.,
372 and H.K. coordinated the experimental work, analyzed the data, and wrote the manuscript,
373 with contributions from all of the authors.

374

375 **ACKNOWLEDGMENTS**

376 We thank all of the laboratory members for their helpful discussion and encouragement.
377 This study was supported in part by Grants-in-Aid for Scientific Research from the
378 Ministry of Education, Culture, Sports, Science, and Technology, Japan (19H01048 to
379 H.K. and 20K17072 to K.M.); the Japan Foundation for Applied Enzymology (VBIC to
380 K.M.); the Miyata Foundation Bounty for Pediatric Cardiovascular Research (K.M.); the
381 SENSHIN Medical Research Foundation (K.M.); the Platform for Dynamic Approaches
382 to Living Systems of the Ministry of Education, Culture, Sports, Science, and Technology,
383 Japan; and the Core Research for Evolutional Science and Technology (CREST) program
384 of the Japan Science and Technology Agency (JST), Japan (JPMJCR13W2).

385

386 **Competing financial interests:** The authors declare that no competing financial
387 interests exist.

388

bioRxiv preprint doi: https://doi.org/10.1101/2022.03.30.486479; this version posted April 1, 2022. The copyright holder for this preprint (which was not certified by peer review) is the author/funder, who has granted bioRxiv a license to display the preprint in perpetuity. It is made available under aCC-BY-NC-ND 4.0 International license.

## REFERENCES

1. Oliver G, Alitalo K. THE LYMPHATIC VASCULATURE: Recent Progress and Paradigms. *Annu Rev Cell Dev Bi*. 2005;21:457–483.

2. Oliver G, Kipnis J, Randolph GJ, Harvey NL. The Lymphatic Vasculature in the 21st Century: Novel Functional Roles in Homeostasis and Disease. *Cell*. 2020;182:270–296.

3. Oliver G. Lymphatic vasculature development. *Nat Rev Immunol*. 2004;4:35–45.

4. Oliver G, Srinivasan RS. Endothelial cell plasticity: how to become and remain a lymphatic endothelial cell. *Development*. 2010;137:363–372.

5. Tammela T, Alitalo K. Lymphangiogenesis: Molecular mechanisms and future promise. *Cell*. 2010;140:460–76.

6. Klaourakis K, Vieira JM, Riley PR. The evolving cardiac lymphatic vasculature in development, repair and regeneration. *Nat Rev Cardiol*. 2021;1–12.

7. Gutierrez-Miranda L, Yaniv K. Cellular Origins of the Lymphatic Endothelium: Implications for Cancer Lymphangiogenesis. *Front Physiol*. 2020;11:577584.

8. Huntington GS, McClure CFW. The anatomy and development of the jugular lymph sacs in the domestic cat (Felis domestica). *Am J Anat*. 1910;10:177–312.

9. Sabin FR. On the origin of the lymphatic system from the veins and the development of the lymph hearts and thoracic duct in the pig. *Am J Anat*. 1902;1:367–389.

10. Srinivasan RS, Dillard ME, Lagutin OV, Lin F-J, Tsai S, Tsai M-J, Samokhvalov IM, Oliver G. Lineage tracing demonstrates the venous origin of the mammalian lymphatic vasculature. *Gene Dev* [Internet]. 2007;21:2422–2432. Available from: http://genesdev.cshlp.org/content/21/19/2422

11. Yang Y, García-Verdugo JM, Soriano-Navarro M, Srinivasan RS, Scallan JP, Singh MK, Epstein JA, Oliver G. Lymphatic endothelial progenitors bud from the cardinal vein and intersomitic vessels in mammalian embryos. *Blood*. 2012;120:2340–2348.

12. Wigle JT, Oliver G. Prox1 Function Is Required for the Development of the Murine Lymphatic System. *Cell*. 1999;98:769–778.

13. Hägerling R, Pollmann C, Andreas M, Schmidt C, Nurmi H, Adams RH, Alitalo K, Andresen V, Schulte-Merker S, Kiefer F. A novel multistep mechanism for initial lymphangiogenesis in mouse embryos based on ultramicroscopy. *Embo J* [Internet]. 2013;32:629–644. Available from: http://emboj.embopress.org/cgi/doi/10.1038/emboj.2012.340

bioRxiv preprint doi: https://doi.org/10.1101/2022.03.30.486479; this version posted April 1, 2022. The copyright holder for this preprint (which was not certified by peer review) is the author/funder, who has granted bioRxiv a license to display the preprint in perpetuity. It is made available under aCC-BY-NC-ND 4.0 International license.

14. Karkkainen MJ, Haiko P, Sainio K, Partanen J, Taipale J, Petrova TV, Jeltsch M, Jackson DG, Talikka M, Rauvala H, Betsholtz C, Alitalo K. Vascular endothelial growth factor C is required for sprouting of the first lymphatic vessels from embryonic veins. *Nat Immunol*. 2004;5:74–80.

15. Koltowska K, Lagendijk AK, Pichol-Thievend C, Fischer JC, Francois M, Ober EA, Yap AS, Hogan BM. Vegfc Regulates Bipotential Precursor Division and Prox1 Expression to Promote Lymphatic Identity in Zebrafish. *Cell Reports*. 2015;13:1828–1841.

16. Nicenboim J, Malkinson G, Lupo T, Asaf L, Sela Y, Mayseless O, Gibbs-Bar L, Senderovich N, Hashimshony T, Shin M, Jerafi-Vider A, Avraham-Davidi I, Krupalnik V, Hofi R, Almog G, Astin JW, Golani O, Ben-Dor S, Crosier PS, Herzog W, Lawson ND, Hanna JH, Yanai I, Yaniv K. Lymphatic vessels arise from specialized angioblasts within a venous niche. *Nature*. 2015;522:56–61.

17. Ny A, Koch M, Schneider M, Neven E, Tong RT, Maity S, Fischer C, Plaisance S, Lambrechts D, Héligon C, Terclavers S, Ciesiolka M, Kälin R, Man WY, Senn I, Wyns S, Lupu F, Brändli A, Vleminckx K, Collen D, Dewerchin M, Conway EM, Moons L, Jain RK, Carmeliet P. A genetic Xenopus laevis tadpole model to study lymphangiogenesis. Nature Publishing Group; 2005.

18. Schneider M, Othman-Hassan K, Christ B, Wilting J. Lymphangioblasts in the avian wing bud. *Dev Dynam*. 1999;216:311–319.

19. Wilting J, Aref Y, Huang R, Tomarev SI, Schweigerer L, Christ B, Valasek P, Papoutsi M. Dual origin of avian lymphatics. *Dev Biol*. 2006;292:165–173.

20. Klotz L, Norman S, Vieira JM, Masters M, Rohling M, Dubé KN, Bollini S, Matsuzaki F, Carr CA, Riley PR. Cardiac lymphatics are heterogeneous in origin and respond to injury. *Nature*. 2015;522:62.

21. Martinez-Corral I, Ulvmar M, Stanczuk L, Tatin F, Kizhatil K, John SWM, Alitalo K, Ortega S, Makinen T. Nonvenous origin of dermal lymphatic vasculature. *Circulation Research*. 2015;

22. Stanczuk L, Martinez-Corral I, Ulvmar MH, Zhang Y, Laviña B, Fruttiger M, Adams RH, Saur D, Betsholtz C, Ortega S, Alitalo K, Graupera M, Mäkinen T. cKit Lineage Hemogenic Endothelium-Derived Cells Contribute to Mesenteric Lymphatic Vessels. *Cell Reports*. 2015;10:1708–1721.

bioRxiv preprint doi: https://doi.org/10.1101/2022.03.30.486479; this version posted April 1, 2022. The copyright holder for this preprint (which was not certified by peer review) is the author/funder, who has granted bioRxiv a license to display the preprint in perpetuity. It is made available under aCC-BY-NC-ND 4.0 International license.

454 23. Pichol-Thievend C, Betterman KL, Liu X, Ma W, Skoczylas R, Lesieur E, Bos FL,
455 Schulte D, Schulte-Merker S, Hogan BM, Oliver G, Harvey NL, Francois M. A blood
456 capillary plexus-derived population of progenitor cells contributes to genesis of the
457 dermal lymphatic vasculature during embryonic development. *Development*.
458 2018;145:dev160184.
459 24. Maruyama K, Miyagawa-Tomita S, Mizukami K, Matsuzaki F, Kurihara H. Isl1-
460 expressing non-venous cell lineage contributes to cardiac lymphatic vessel
461 development. *Dev Biol*. 2019;452:134–143.
462 25. Lioux G, Liu X, Temiño S, Oxendine M, Ayala E, Ortega S, Kelly RG, Oliver G,
463 Torres M. A Second Heart Field-Derived Vasculogenic Niche Contributes to Cardiac
464 Lymphatics. *Dev Cell*. 2020;
465 26. Diogo R, Kelly RG, Christiaen L, Levine M, Ziermann JM, Molnar JL, Noden DM,
466 Tzahor E. A new heart for a new head in vertebrate cardiopharyngeal evolution. *Nature*.
467 2015;520:466–473.
468 27. Tirosh-Finkel L, Elhanany H, Rinon A, Tzahor E. Mesoderm progenitor cells of
469 common origin contribute to the head musculature and the cardiac outflow tract.
470 *Development*. 2006;133:1943–1953.
471 28. Harel I, Nathan E, Tirosh-Finkel L, Zigdon H, Guimarães-Camboa N, Evans SM,
472 Tzahor E. Distinct Origins and Genetic Programs of Head Muscle Satellite Cells. *Dev*
473 *Cell*. 2009;16:822–832.
474 29. Tzahor E, Evans SM. Pharyngeal mesoderm development during embryogenesis:
475 implications for both heart and head myogenesis. *Cardiovasc Res*. 2011;91:196–202.
476 30. Nathan E, Monovich A, Tirosh-Finkel L, Harrelson Z, Rousso T, Rinon A, Harel I,
477 Evans SM, Tzahor E. The contribution of Islet1-expressing splanchnic mesoderm cells
478 to distinct branchiomeric muscles reveals significant heterogeneity in head muscle
479 development. *Development*. 2008;135:647–57.
480 31. Adachi N, Bilio M, Baldini A, Kelly RG. Cardiopharyngeal mesoderm origins of
481 musculoskeletal and connective tissues in the mammalian pharynx. *Development*.
482 2020;147:dev185256.
483 32. Lescroart F, Kelly RG, Garrec J-FL, Nicolas J-F, Meilhac SM, Buckingham M.
484 Clonal analysis reveals common lineage relationships between head muscles and second
485 heart field derivatives in the mouse embryo. *Dev Camb Engl*. 2010;137:3269–79.

bioRxiv preprint doi: https://doi.org/10.1101/2022.03.30.486479; this version posted April 1, 2022. The copyright holder for this preprint (which was not certified by peer review) is the author/funder, who has granted bioRxiv a license to display the preprint in perpetuity. It is made available under aCC-BY-NC-ND 4.0 International license.

33. Engleka KA, Manderfield LJ, Brust RD, Li L, Cohen A, Dymecki SM, Epstein JA. Islet1 Derivatives in the Heart Are of Both Neural Crest and Second Heart Field Origin. *Circ Res*. 2012;110:922–926.

34. Iwano T, Masuda A, Kiyonari H, Enomoto H, Matsuzaki F. Prox1 postmitotically defines dentate gyrus cells by specifying granule cell identity over CA3 pyramidal cell fate in the hippocampus. *Development*. 2012;139:3051–62.

35. Stone OA, Stainier DYR. Paraxial Mesoderm Is the Major Source of Lymphatic Endothelium. *Dev Cell*. 2019;

36. Johnson NC, Dillard ME, Baluk P, McDonald DM, Harvey NL, Frase SL, Oliver G. Lymphatic endothelial cell identity is reversible and its maintenance requires Prox1 activity. *Gene Dev*. 2008;22:3282–3291.

37. Milgrom-Hoffman M, Harrelson Z, Ferrara N, Zelzer E, Evans SM, Tzahor E. The heart endocardium is derived from vascular endothelial progenitors. *Development*. 2011;138:4777–4787.

38. Nomaru H, Liu Y, Bono CD, Righelli D, Cirino A, Wang W, Song H, Racedo SE, Dantas AG, Zhang L, Cai C-L, Angelini C, Christiaen L, Kelly RG, Baldini A, Zheng D, Morrow BE. Single cell multi-omic analysis identifies a Tbx1-dependent multilineage primed population in murine cardiopharyngeal mesoderm. *Nat Commun*. 2021;12:6645.

39. Wang W, Niu X, Stuart T, Jullian E, Mauck WM, Kelly RG, Satija R, Christiaen L. A single-cell transcriptional roadmap for cardiopharyngeal fate diversification. *Nat Cell Biol*. 2019;21:674–686.

40. Eng TC, Chen W, Okuda KS, Misa JP, Padberg Y, Crosier KE, Crosier PS, Hall CJ, Schulte-Merker S, Hogan BM, Astin JW. Zebrafish facial lymphatics develop through sequential addition of venous and non-venous progenitors. *Embo Rep*. 2019;20.

41. Gancz D, Raftrey BC, Perlmoter G, Marín-Juez R, Semo J, Matsuoka RL, Karra R, Raviv H, Moshe N, Addadi Y, Golani O, Poss KD, Red-Horse K, Stainier DY, Yaniv K. Distinct origins and molecular mechanisms contribute to lymphatic formation during cardiac growth and regeneration. *Elife*. 2019;8:e44153.

42. Perkins JA, Manning SC, Tempero RM, Cunningham MJ, Edmonds JL, Hoffer FA, Egbert MA. Lymphatic malformations: Review of current treatment. *Otolaryngology - Head Neck Surg*. 2010;142:795-803.e1.

bioRxiv preprint doi: https://doi.org/10.1101/2022.03.30.486479; this version posted April 1, 2022. The copyright holder for this preprint (which was not certified by peer review) is the author/funder, who has granted bioRxiv a license to display the preprint in perpetuity. It is made available under aCC-BY-NC-ND 4.0 International license.

518 43. Blesinger H, Kaulfuß S, Aung T, Schwoch S, Prantl L, Rößler J, Wilting J, Becker
519 J. PIK3CA mutations are specifically localized to lymphatic endothelial cells of
520 lymphatic malformations. *Plos One*. 2018;13:e0200343.
521 44. Cai C-L, Liang X, Shi Y, Chu P-H, Pfaff SL, Chen J, Evans S. Isl1 Identifies a
522 Cardiac Progenitor Population that Proliferates Prior to Differentiation and Contributes
523 a Majority of Cells to the Heart. *Dev Cell*. 2003;5:877–889.
524 45. Laugwitz K-L, Moretti A, Lam J, Gruber P, Chen Y, Woodard S, Lin L-Z, Cai C-L,
525 Lu MM, Reth M, Platoshyn O, Yuan JX-J, Evans S, Chien KR. Postnatal isl1+
526 cardioblasts enter fully differentiated cardiomyocyte lineages. *Nature*. 2005;433:647–
527 653.
528 46. Jiang X, Rowitch DH, Soriano P, McMahon AP, Sucov HM. Fate of the mammalian
529 cardiac neural crest. *Development*. 2000;127:1607–1616.
530 47. Biressi S, Bjornson CRR, Carlig PMM, Nishijo K, Keller C, Rando TA. Myf5
531 expression during fetal myogenesis defines the developmental progenitors of adult
532 satellite cells. *Dev Biol*. 2013;379:195–207.
533 48. Srinivas S, Watanabe T, Lin C-S, William CM, Tanabe Y, Jessell TM, Costantini F.
534 Cre reporter strains produced by targeted insertion of EYFP and ECFP into the
535 ROSA26 locus. *Bmc Dev Biol*. 2001;1:4.
536 49. Madisen L, Zwingman TA, Sunkin SM, Oh SW, Zariwala HA, Gu H, Ng LL,
537 Palmiter RD, Hawrylycz MJ, Jones AR, Lein ES, Zeng H. A robust and high-
538 throughput Cre reporting and characterization system for the whole mouse brain. *Nat*
539 *Neurosci*. 2010;13:133–140.
540 50. Kisanuki YY, Hammer RE, Miyazaki J, Williams SC, Richardson JA, Yanagisawa
541 M. Tie2-Cre Transgenic Mice: A New Model for Endothelial Cell-Lineage Analysis in
542 Vivo. *Dev Biol*. 2001;230:230–242.
543
544

bioRxiv preprint doi: https://doi.org/10.1101/2022.03.30.486479; this version posted April 1, 2022. The copyright holder for this preprint (which was not certified by peer review) is the author/funder, who has granted bioRxiv a license to display the preprint in perpetuity. It is made available under aCC-BY-NC-ND 4.0 International license.

## Figure legends

**Figure 1. Isl1$^+$ lineages contribute to cranial and cardiac lymphatic vessels**

(**A-G**) Sagittal sections of Isl1-Cre; R26RtdTomato embryos, in which PECAM, tdTomato, and VEGFR3 were labeled at E16.5, are shown. (**A-F**) tdTomato colocalized with PECAM/VEGFR3 (white arrows) and PECAM (yellow arrows) in and around the larynx (**B**), the skin of the lower jaw (**C**), the tongue (**D**), and the cardiac outflow tracts (**F**) (n=3). (**G**) tdTomato did not colocalize with VEGFR3 in the LECs on the dorsal side of the ventricles (white arrowhead, n=3). (**H**) The results of quantitative analysis of the percentage of tdTomato$^+$/VEGFR3$^+$ lymphatic vessels among all VEGFR3$^+$ lymphatic vessels are shown. (**I-O**) Sagittal sections of Wnt1-Cre; R26ReYFP embryos, in which PECAM, eYFP, and VEGFR3 were labeled at E16.5, are shown. There were no eYFP$^+$/VEGFR3$^+$ lymphatic vessels in or around the larynx, the skin of the lower jaw, the tongue, or the heart (the white arrowheads indicate cardiac lymphatic vessels around the cardiac outflow tracts and the dorsal side of the ventricles; n=3). Each dot represents a value obtained from one sample. L, larynx; T, tongue; Ao, aorta; PA, pulmonary artery; V, ventricle; Scale bars, 100 μm **(B-D, F, G, J-L, N, O)**, 1 mm **(A, E, I, M)**

**Figure 2. The differentiation of Isl1$^+$ CPM cells into LECs occurs during the early embryonic period**

(**A-G, I-O**) Sagittal sections of Isl1-MerCreMer; R26RtdTomato embryos, in which PECAM, tdTomato, and VEGFR3 were labeled at E16.5, are shown. Tamoxifen was administered at E8.5 (**A-G**) or E11.5 (**I-O**). (**A-G**) Both tdTomato$^+$ (white arrows) and tdTomato$^-$ (white arrowheads) lymphatic vessels were observed in and around the larynx (**B**), the skin of the lower jaw (**C**), the tongue (**D**), and the cardiac outflow tracts (**F**) (n=5). (**G**) tdTomato did not colocalize with VEGFR3 in the LECs on the dorsal side of the ventricles (white arrowhead, n=5). (**I-O**) Almost all of the VEGFR3$^+$ lymphatic vessels in and around the larynx (**J**), the skin of the lower jaw (**K**), the tongue (**L**), the cardiac outflow tracts (**N**), and the dorsal side of the ventricles (**O**) were tdTomato$^-$ (white arrows, n=3). (**H, P**) The results of a quantitative analysis of the percentage of tdTomato$^+$/VEGFR3$^+$ lymphatic vessels among all VEGFR3$^+$ lymphatic vessels are shown. Tamoxifen was administered at E8.5 (**H**) or E11.5 (**P**). Each dot represents a value obtained from one sample. L, larynx; T, tongue; Ao, aorta; PA, pulmonary artery; V, ventricle; Scale bars, 100 μm **(B-D, F, G, J-L, N, O)**, 1 mm **(A, E, I, M)**

bioRxiv preprint doi: https://doi.org/10.1101/2022.03.30.486479; this version posted April 1, 2022. The copyright holder for this preprint (which was not certified by peer review) is the author/funder, who has granted bioRxiv a license to display the preprint in perpetuity. It is made available under aCC-BY-NC-ND 4.0 International license.

**Figure 3. Isl1$^+$ CPM cells contribute to cardiac lymphatic vessel development**

(**A-H**) Whole-mount confocal images of Isl1-MerCreMer; R26ReYFP hearts, in which PECAM, eYFP, and VEGFR3 were labeled at E16.5, are shown. Tamoxifen was administered at E8.5 (**A-D**) or E11.5 (**E-H**). (**A-D**) Many eYFP$^+$ cells were observed around the cardiac outflow tracts, and they contributed to lymphatic vessels (white arrow) (n=9/9 hearts (100%)) (**A-C**). (**D**) There were no eYFP$^+$ lymphatic vessels on the dorsal side of the ventricles (n=9/9 hearts (100%)). The cardiac nerves were also positive for eYFP after tamoxifen treatment at E8.5 (white arrowhead) (**D**). (**E-H**) Fewer eYFP$^+$ cells were observed around the cardiac outflow tracts (**E-G**), and there were no eYFP$^+$ lymphatic vessels around the cardiac outflow tracts (**F**) or on the dorsal side of the ventricles (n=0/8) (**H**). Ao, aorta; PA, pulmonary artery; Scale bars, 100 μm **(A-C, E-G)**, 500 μm **(D, H)**

**Figure 4. The spatiotemporal development of Isl1$^+$ CPM-derived LECs**

(**A-G**) Whole-mount and sagittal section images of Isl1-Cre; R26ReYFP embryos, in which PECAM, eYFP, and Prox1 were labeled at E11.5, E12.0, or E14.5, are shown. (**A, B**) eYFP$^+$/Prox1$^+$ cells were observed around the cores of the first and second pharyngeal arches at E11.5 (white arrowheads). (**C, D**) eYFP$^+$/Prox1$^+$ LECs migrated from the first and second pharyngeal arches to the lymph sac-forming domain (white dotted region) adjacent to the anterior cardinal vein at E12.0 (white arrows). (**E-G**) Some of the eYFP$^+$/Prox1$^+$ LECs expressed PECAM and formed lymphatic capillaries in the lower jaw and tongue at E14.5 (white arrows). (**H-N**) Whole-mount and sagittal section images of Isl1-MerCreMer; R26ReYFP embryos, in which PECAM, eYFP, and Prox1 were labeled at E12.0, are shown. Tamoxifen was administered at E8.5 (**H-L**) or E9.5 (**M and N**). (**I**) eYFP$^+$/Prox1$^+$ LECs (white arrows) migrated from the first and second pharyngeal arches to the lymph sac-forming domain (white dotted region) at E12.0. (**J**) There were no eYFP$^+$/Prox1$^+$ cells in or around the cardinal vein (n=4). (**K-N**) eYFP$^+$/Prox1$^+$/PECAM$^+$ LECs were seen in the first and second pharyngeal arches of the embryos at E12.0, when tamoxifen was administered at E8.5 or E9.5 (white arrows), although the number of these cells was decreased in the E9.5 group (**M and N**). (**O**) The results of a quantitative analysis of the percentage of eYFP$^+$/Prox1$^+$ cells among Prox1$^+$ cells in the first and second pharyngeal arches at E12.0 after tamoxifen treatment at E8.5

bioRxiv preprint doi: https://doi.org/10.1101/2022.03.30.486479; this version posted April 1, 2022. The copyright holder for this preprint (which was not certified by peer review) is the author/funder, who has granted bioRxiv a license to display the preprint in perpetuity. It is made available under aCC-BY-NC-ND 4.0 International license.

or E9.5 are shown. All of the data are presented as the mean±SEM, and statistical analyses were performed using the non-parametric Mann-Whitney *u*-test. V, ventricle; PA1, first pharyngeal arch; PA2, second pharyngeal arch; CV, cardinal vein; LS, lymph sac-forming domain; L, liver; T, tongue; RA, right atrium; OFT, cardiac outflow tract; Scale bars, 100 μm **(A, B, D, F, G, I, J, L, N)**, 500 μm **(C, E, H, K, M)**; ***P*<0.01

**Figure 5. The inactivation of Prox1 in Isl1$^{+}$ lineages confirmed the contribution of the CPM to cranial lymphatic vessel development**

(**A-J'''**) Coronal sections of Isl1-Cre; Prox1$^{fl/+}$ and Isl1-Cre; Prox1$^{fl/fl}$ mouse embryos, in which PECAM, eYFP, and VEGFR3 were labeled at E16.5, are shown. **(J)** The number of eYFP$^{-}$/VEGFR3$^{+}$ lymphatic vessels in facial skin was increased in the Isl1-Cre; Prox1$^{fl/fl}$ homozygous mice (white arrows). (**K-R**) The results of quantitative analysis of lymphatic vessel formation in the tongue (**K-N**) and facial skin (**O-R**) are shown. All the data are presented as the mean±SEM, and statistical analyses were performed using the non-parametric Mann-Whitney *u*-test. Each dot represents a value obtained from one sample. ***P*<0.01; T, tongue; Scale bars, 100 μm **(B-E, G-J)**, 1 mm **(A, F)**

**Figure 6**. **Prox1 knockdown in Tie2$^{+}$ lineages revealed regional differences in lymphatic vessel development**

(**A-F**) Sagittal sections of Tie2-Cre; Prox1$^{fl/+}$ or Tie2-Cre; Prox1$^{fl/fl}$ mouse embryos, in which PECAM, eGFP, LYVE1, and DAPI were labeled at E16.5, are shown. (**A, B**) In the tongue, the number of LYVE1$^{-}$/eGFP$^{+}$/PECAM$^{+}$ cells in lymphatic vessels was increased in the Tie2-Cre; Prox1$^{fl/fl}$ embryos (white arrows). (**C, D**) In the skin of the lower jaw, the contribution of eGFP$^{+}$ cells to lymphatic vessels was small in both the Tie2-Cre; Prox1$^{fl/+}$ and Tie2-Cre; Prox1$^{fl/fl}$ embryos (white arrows). (**E, F**) LYVE1$^{-}$/eGFP$^{+}$/PECAM$^{+}$ cells were observed in the back skin of the Tie2-Cre; Prox1$^{fl/fl}$ embryos (white arrows). Scale bars, 100 μm (**A-F**)

**Figure 7. Lymphatic endothelial cells are derived from two distinct origins**

Schematic representation of the origins of LECs. LECs are mainly derived from cardinal veins (red dots) and the CPM (green dots).

bioRxiv preprint doi: https://doi.org/10.1101/2022.03.30.486479; this version posted April 1, 2022. The copyright holder for this preprint (which was not certified by peer review) is the author/funder, who has granted bioRxiv a license to display the preprint in perpetuity. It is made available under aCC-BY-NC-ND 4.0 International license.

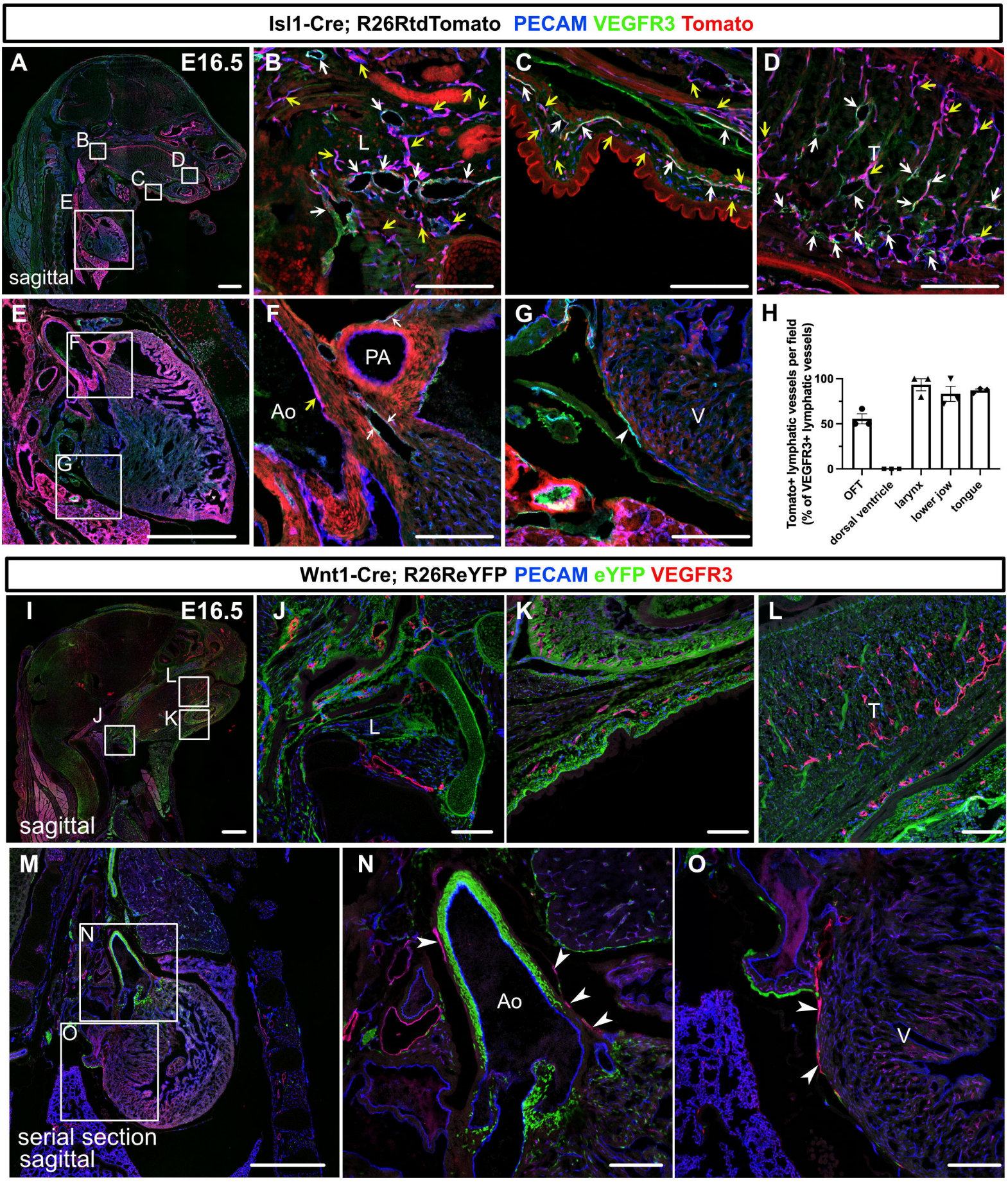

bioRxiv preprint doi: https://doi.org/10.1101/2022.03.30.486479; this version posted April 1, 2022. The copyright holder for this preprint (which was not certified by peer review) is the author/funder, who has granted bioRxiv a license to display the preprint in perpetuity. It is made available under aCC-BY-NC-ND 4.0 International license.

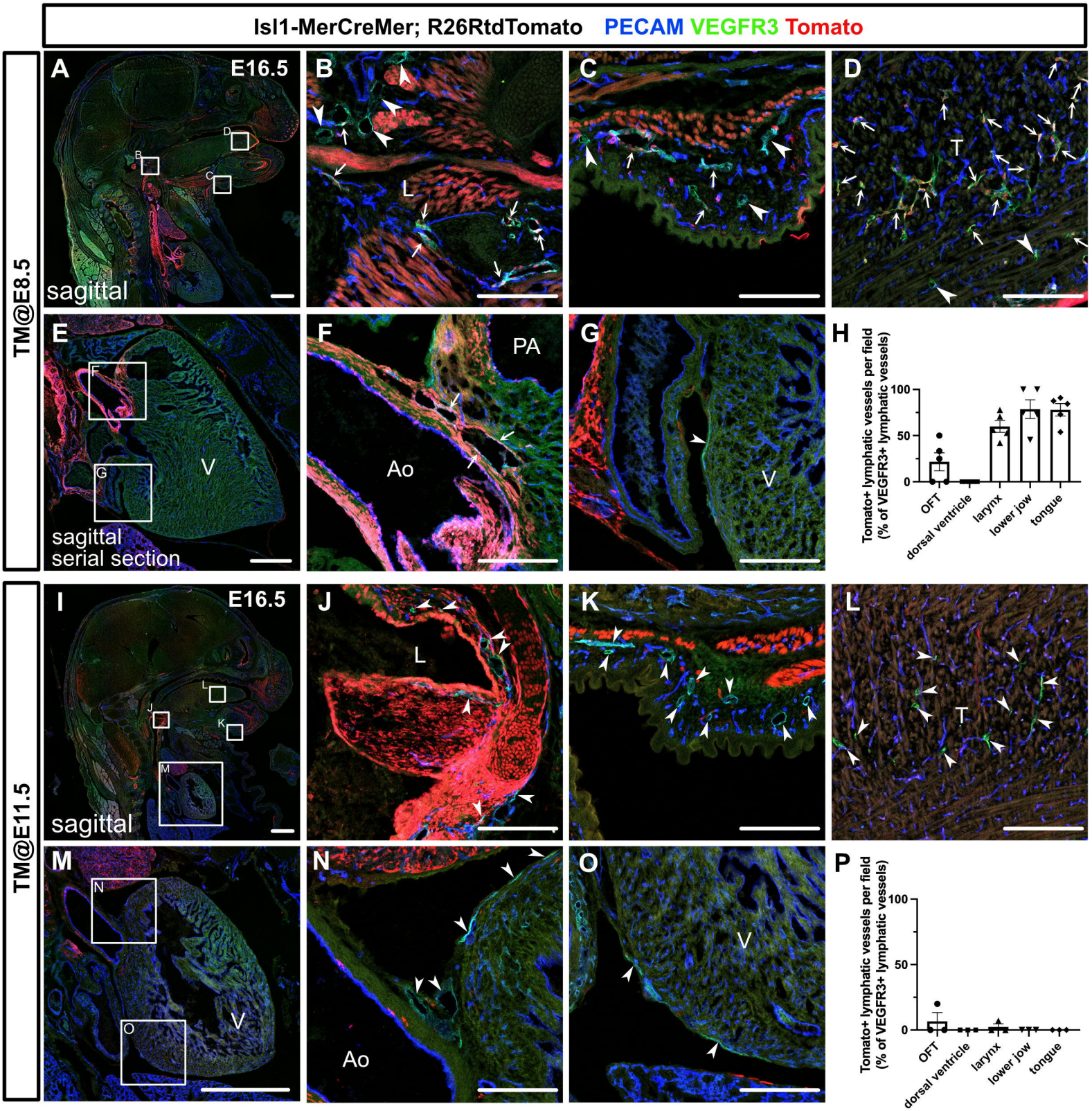

bioRxiv preprint doi: https://doi.org/10.1101/2022.03.30.486479; this version posted April 1, 2022. The copyright holder for this preprint (which was not certified by peer review) is the author/funder, who has granted bioRxiv a license to display the preprint in perpetuity. It is made available under aCC-BY-NC-ND 4.0 International license.

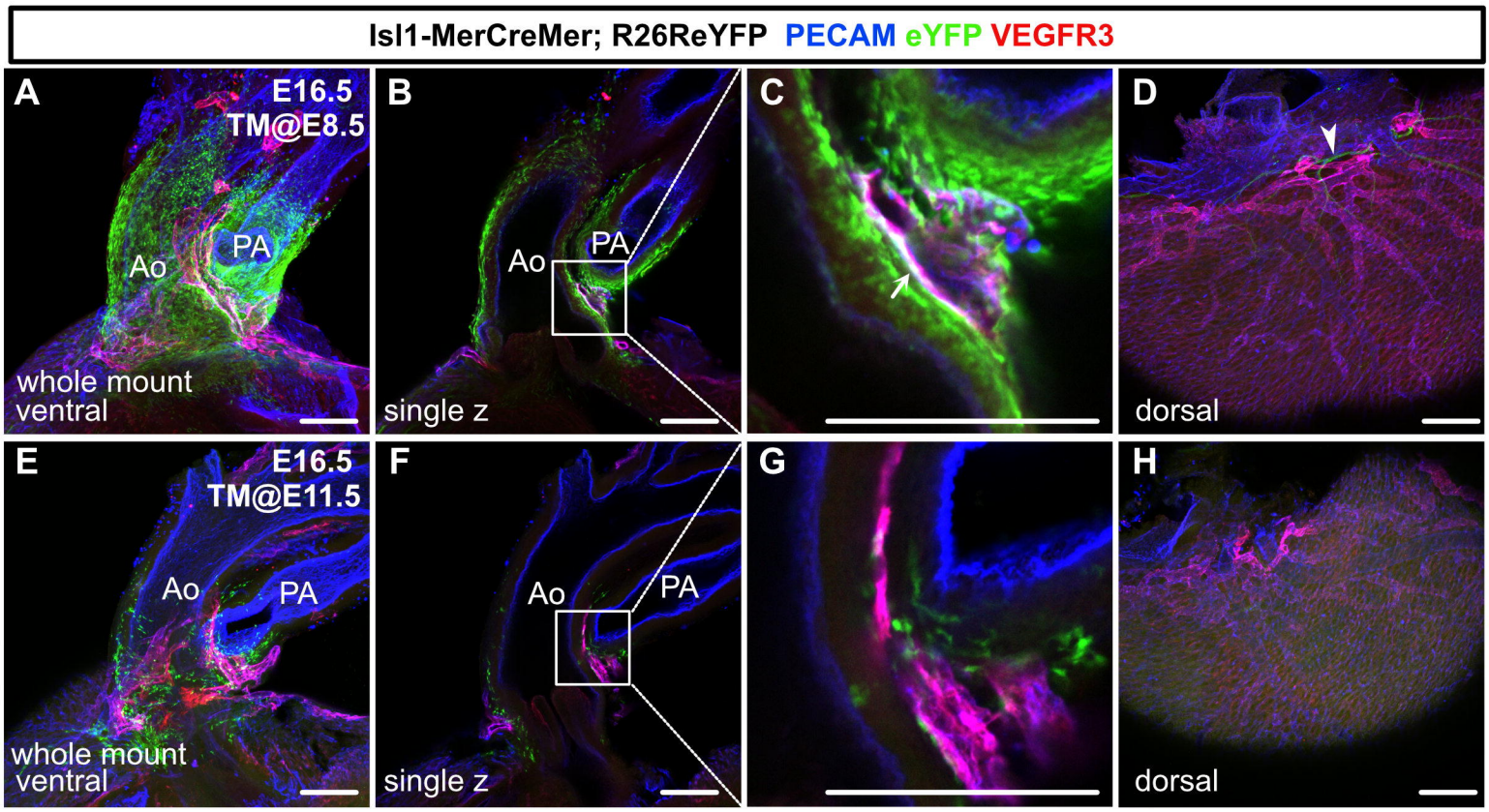

bioRxiv preprint doi: https://doi.org/10.1101/2022.03.30.486479; this version posted April 1, 2022. The copyright holder for this preprint (which was not certified by peer review) is the author/funder, who has granted bioRxiv a license to display the preprint in perpetuity. It is made available under aCC-BY-NC-ND 4.0 International license.

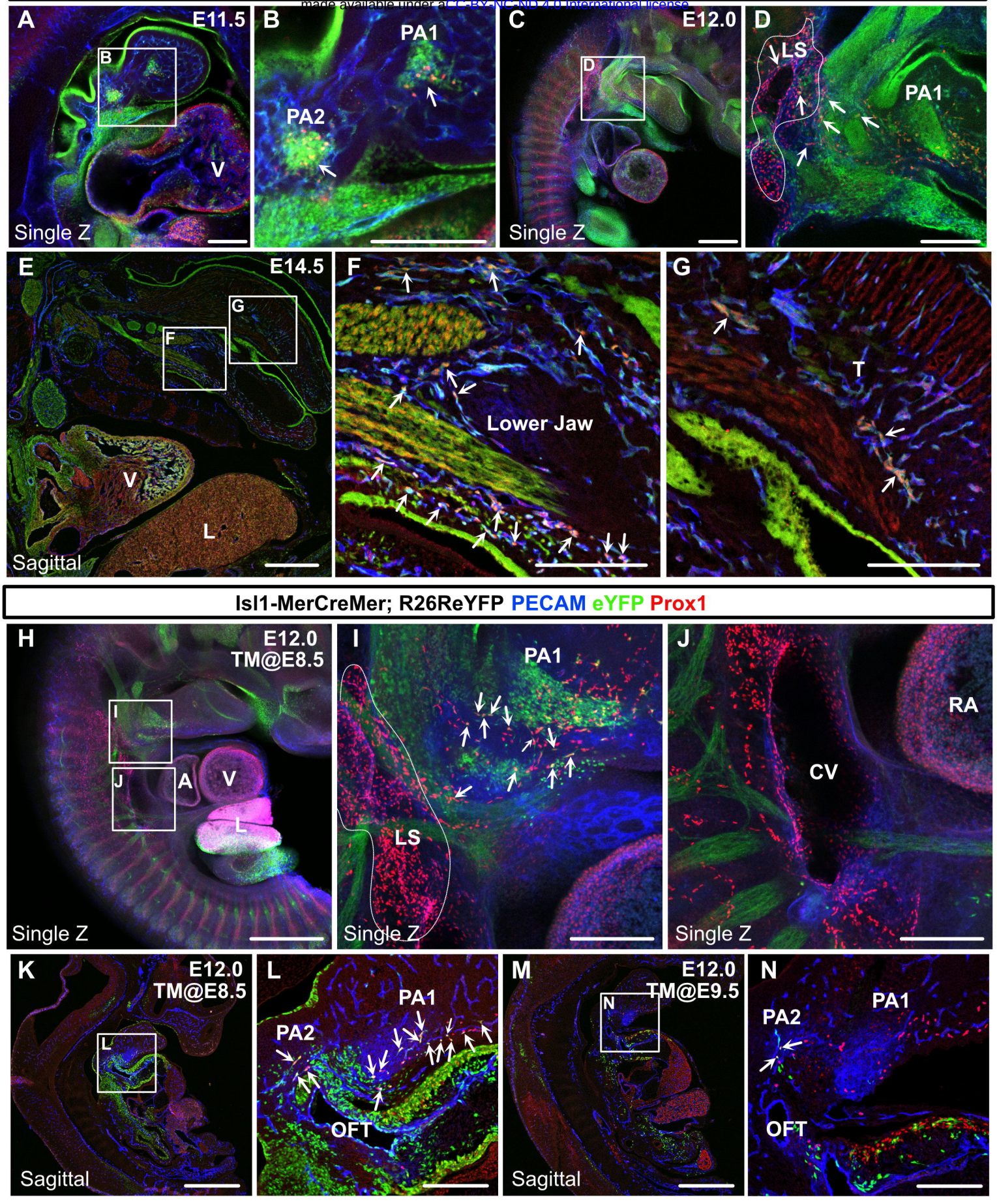

bioRxiv preprint doi: https://doi.org/10.1101/2022.03.30.486470; this version posted April 1, 2022. The copyright holder for this preprint (which was not certified by peer review) is the author/funder, who has granted bioRxiv a license to display the preprint in perpetuity. It is made available under aCC-BY-NC-ND 4.0 International license.

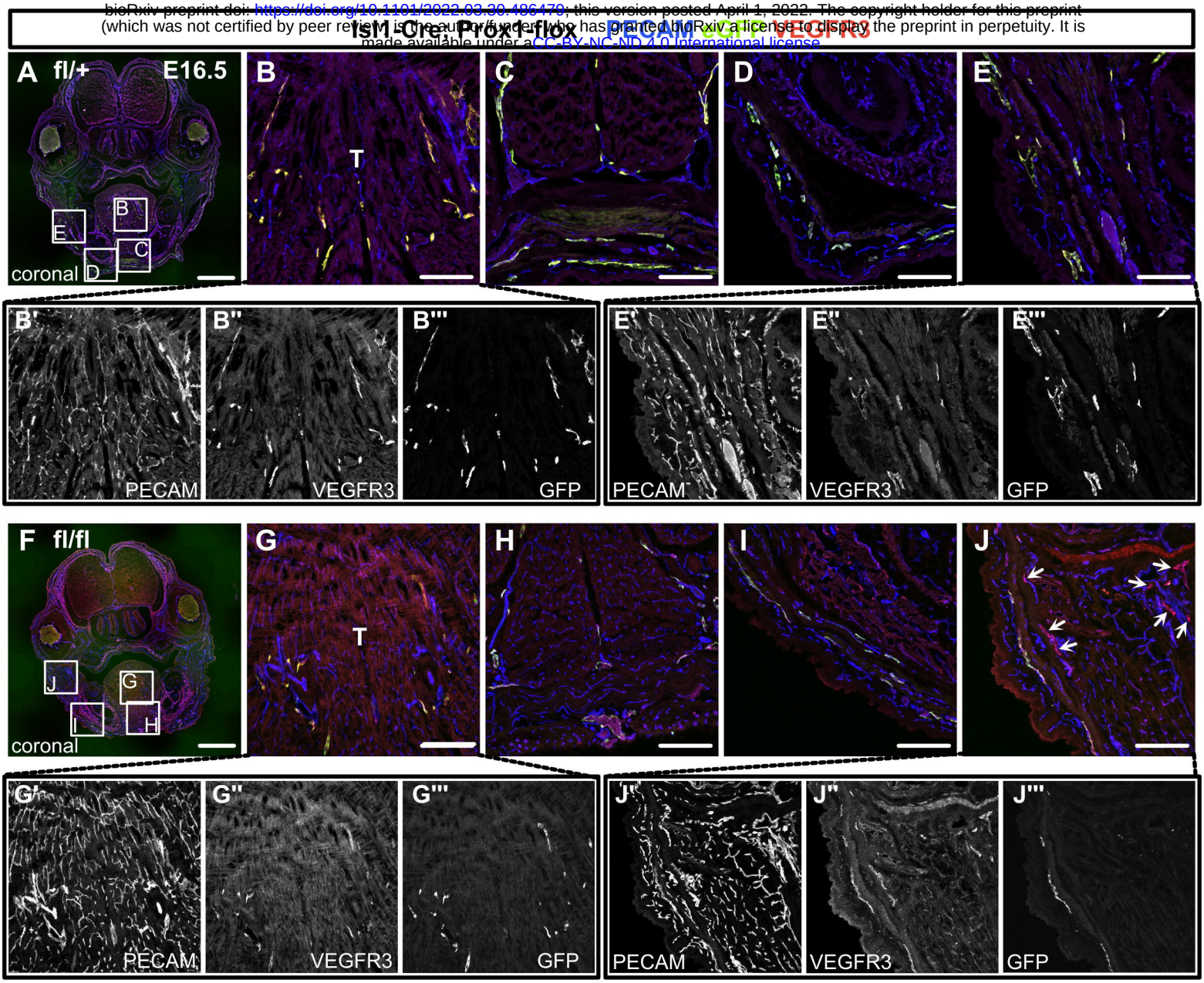


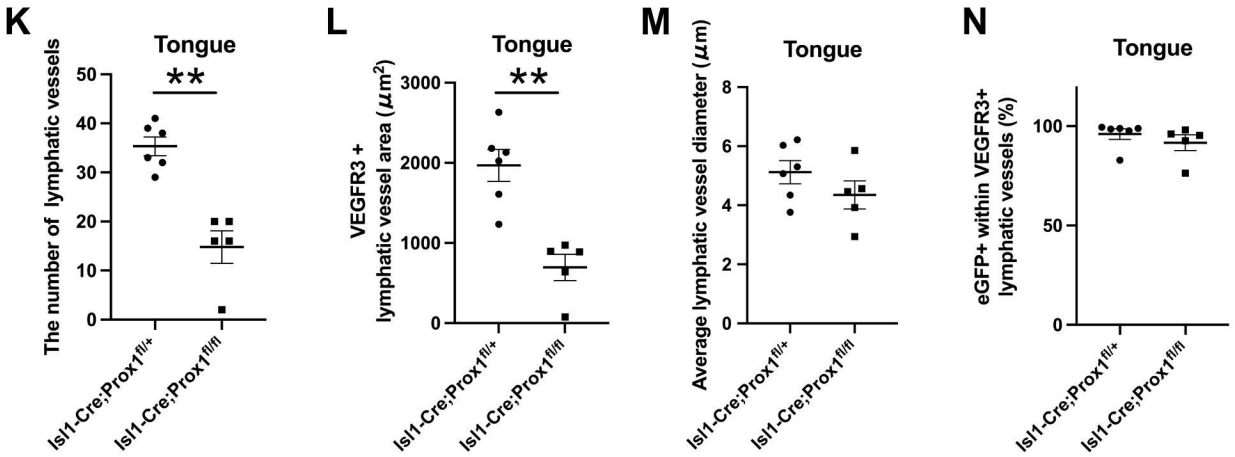


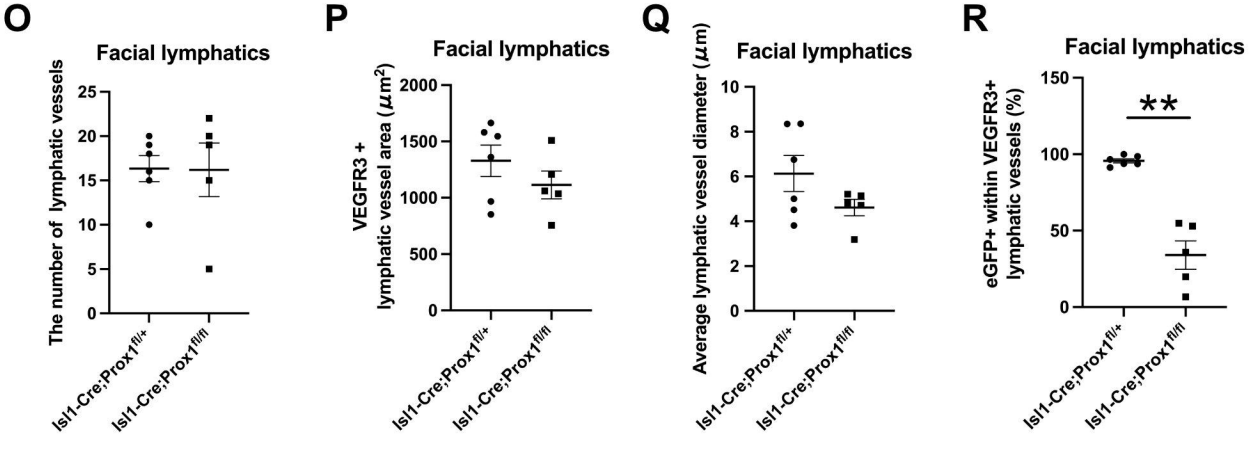

bioRxiv preprint doi: https://doi.org/10.1101/2022.03.30.486479; this version posted April 1, 2022. The copyright holder for this preprint (which was not certified by peer review) is the author/funder, who has granted bioRxiv a license to display the preprint in perpetuity. It is made available under aCC-BY-NC-ND 4.0 International license.

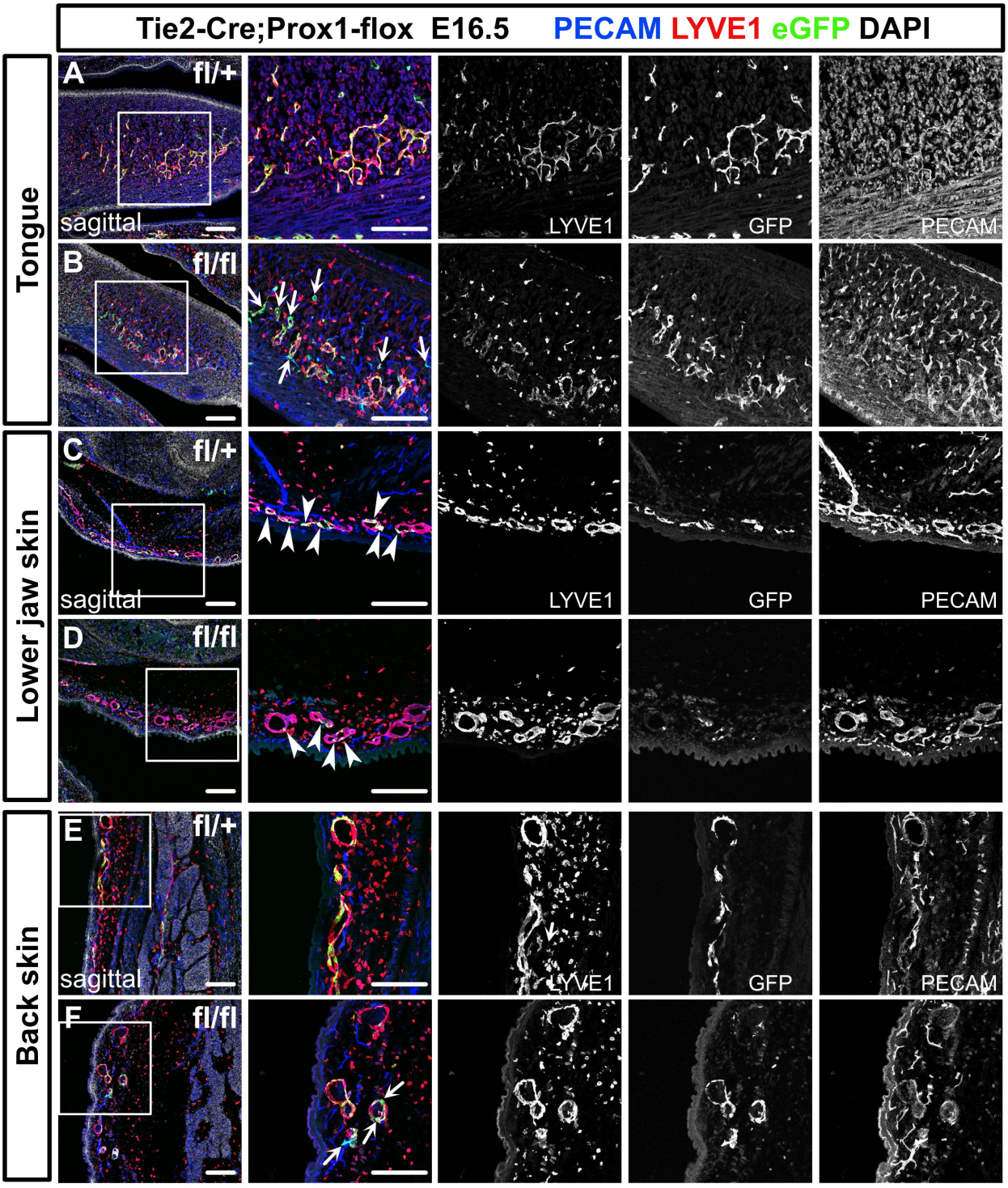

bioRxiv preprint doi: https://doi.org/10.1101/2022.03.30.486479; this version posted April 1, 2022. The copyright holder for this preprint (which was not certified by peer review) is the author/funder, who has granted bioRxiv a license to display the preprint in perpetuity. It is made available under aCC-BY-NC-ND 4.0 International license.

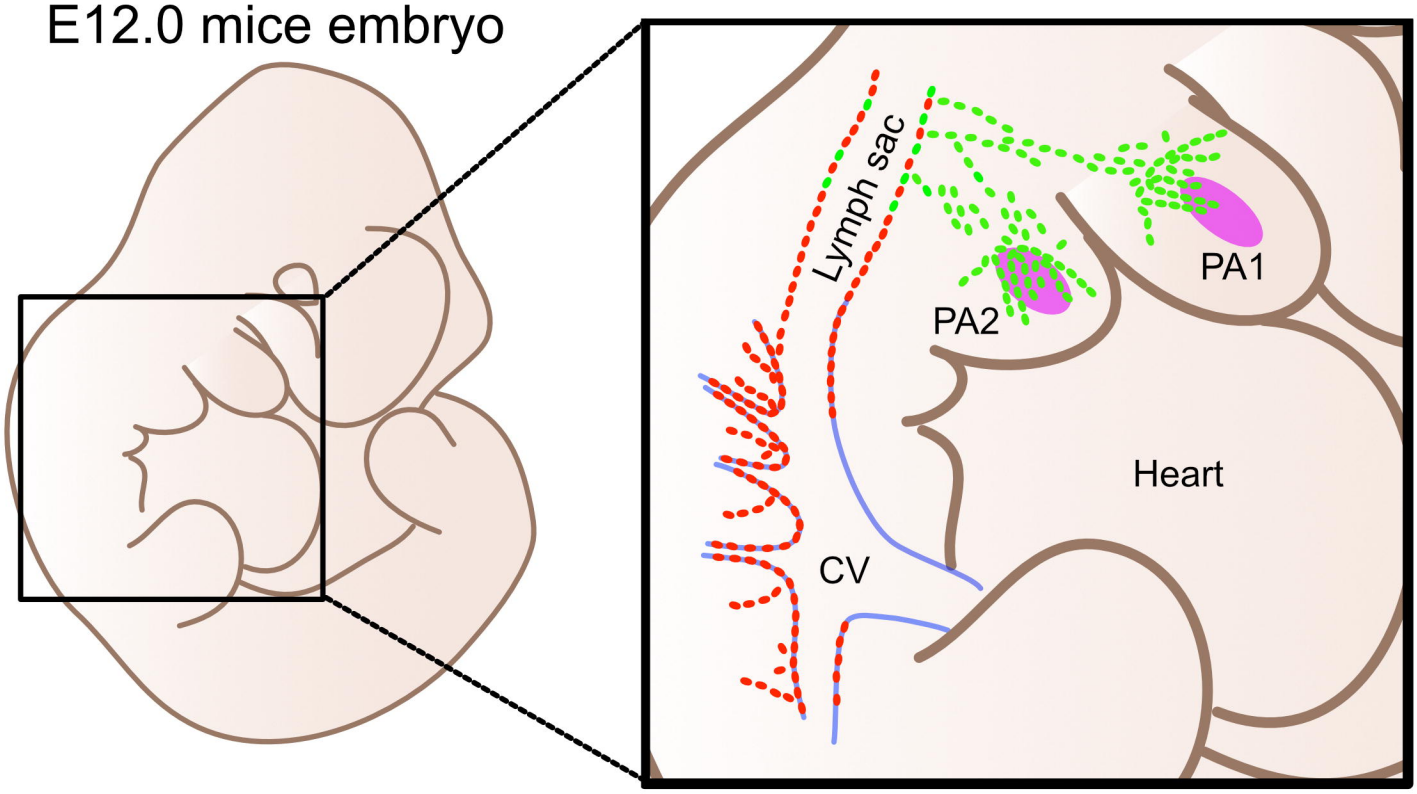


Lymphatic endothelial cells are mainly derived from

1. Cardinal vein (●).
2. **Cardiopharyngeal mesoderm (●).**